

***In Situ* and Real-Time Monitoring of Powder-Bed AM by Combining Acoustic Emission and Artificial Intelligence**

K. Wasmer^(✉), C. Kenel, C. Leinenbach, and S.A. Shevchik

Laboratory for Advanced Materials Processing,
Empa – Swiss Federal Laboratories for Materials Science and Technology,
Thun, Switzerland
kilian.wasmer@empa.ch

Abstract. At present, the quality control in additive manufacturing is diligently based on temperature of the process zone or high resolution imaging. Hence, various sensors such as pyrometers, photo diodes and matrix CCD detectors are used. The discrepancies in temperature measurements and the real temperature distribution inside the powder medium reduce the reliability of this method. The high resolution imaging monitors the quality *post factum*, after a part is manufactured. So far, no methods are known to monitor the quality of additive manufacturing *in situ* and in real-time. To achieve the goal of accurate real-time quality control, we propose an approach that relies on acoustic emission, which is further analyzed within artificial intelligence framework. We show that the additive manufacturing process has a number of unique acoustic signatures that can be detected, extracted and interpreted in terms of quality.

In this contribution, the processing parameters for the selective laser melting of a 316L steel were modified to create a specimen consisting of sections with three quality levels. During the process, the acoustic emission data were acquired and then processed prior validation. The confidence level achieved in the classification is 79–84% that demonstrates the applicability of this approach for *in situ* and real-time quality monitoring in additive manufacturing. Finally, the proposed method is very flexible in terms of realization and can be integrated in any additive manufacturing machine.

Keywords: Additive manufacturing · Quality control · Acoustic emission · Fiber optical sensors · Artificial intelligence

1 Introduction

In recent years, additive manufacturing (AM) has attracted considerable attention from the industrial world [1, 2]. The main reason is that unlike conventional material removal methods, AM is based on additive material method [3]. This manufacturing strategy has placed AM as one of the most promising future technologies [4] and is recognized, today and by many, as the next industrial revolution [5]. The main reason for this is that AM reduces the geometrical constraints of the parts as compared to conventional manufacturing [5, 6].

Several AM technologies exist such as Laser Cusing, Direct Metal Laser Melting, Laser Metal Fusing or Selective Laser Melting (SLM) [7]. In this work, we focused on SLM technology, which is a powder bed AM technology allowing building highly complex 3D geometries layer by layer parts from an alloy powder. This technology has been successfully applied for fast prototyping of unique workpieces and for production of small series of individualized products [7, 8].

Unfortunately, the high expectations are not completely fulfilled as AM is not matured enough. The reason is in the high sensitivity of the AM process to different factors, such as laser parameters, laser optics, mechanical and optical material properties, particles configuration of the powder in the melt zone, etc. [9–11]. Hence, any small changes can have a direct impact on the part quality in terms of pronounced porosity, cracking and accumulation of residual stress inside a part [12]. Under such circumstances, it is obvious that the repeatability of AM processes are limited, preventing the technology from being used in a much wider range. A probable way out of this situation is the development of *in situ* and real-time quality monitoring and control of the part quality [12]. The challenges in such a development are in the complex underlying physics that require interdisciplinary investigations in materials, laser-matter interactions, optical properties of powders and heat propagation [6]. The lack of this knowledge prevents the design of quality monitoring systems [9–12].

At present, the two most common approach for quality monitoring is based on temperature measurements of the process zone and this information is used to keep the melt pool stable [12–14]. The other methodology is based on the image processing of the surface of the manufactured layer [12, 13, 15–18]. Both approaches have drawbacks. The temperature measurements are taken from the surface and no precise estimation of its propagation in depth exists so that the inaccuracies lead to uncontrollable formation of defects. The image processing is a *post mortem* analysis that is carried out after the workpiece is manufactured and no quality improvements are possible [12, 13, 15–18]. Hence, there is a consensus among scientists and industries that there is a lack in reproducibility when producing a workpiece in mass production [1, 3, 12–18].

In recent years, acoustic emission (AE) has been involved for quality monitoring of some industrial processes [19, 20]. Its advantages are in the fast data acquisition and processing since it is represented by 1D sequences, whereas imaging is 2D. Additionally, cutting edge AE sensors, in particular fiber Bragg grating (FBG), are known to be highly sensitive [20, 21]. Thus, some attempts to use either active or passive AE for AM process exist in the literature [22–26] but no link was found between the AE and the quality of the part.

In recent years, significant progresses have been made in terms of artificial intelligence (AI). In a first try of combining FBG sensor and artificial intelligence, we evaluated spectral convolutional neural networks (SCNN) and conventional CNN [27]. The classification accuracy for SCNN was higher than CNN and ranged between 83 to 89% for the three quality levels. In this contribution, a convolutional neural network (CNN) was employed since it is top notch method used in acoustic signals processing, principally for speech recognition [28]. CNN incorporates self-features extraction layers that produce the optimal features for a given task. This makes CNN very interesting for industrial applications as CNN is able to self-optimize the algorithm with a minimum human participation.

2 Experimental Setup, Material and Acoustic Datasets

The experiments were performed on an industrial Concept M2 machine (Concept Laser GmbH, Germany). This machine is based on a selective laser melting (SLM) process. The machine had a fiber laser with wavelength of 1071 nm, a spot diameter of 90 μm , a beam quality $M^2 = 1.02$ and operating in continuous mode. The powder had a particle size distribution ranging from 10 to 45 μm and was made of CL20ES stainless steel (1.4404/316L).

The part produced was a cube with dimensions $10 \times 10 \times 20 \text{ mm}^3$ shown in Fig. 1a. The process was carried out under N_2 atmosphere so that the O_2 content stayed below 1% during the entire process. Except the laser scanning velocity, the process parameters were kept constant. The laser power P was 125 W, the hatching distance h was 0.105 mm and the layer thickness t was 0.03 mm. Three laser scanning speeds were selected and they were 300, 500 and 800 mm/s. The corresponding energy densities were calculated to be 132, 79, 50 J/mm^3 [29]. The scanning regimes resulted in three pore concentrations inside the part, which was measured on cross-sections via visual inspection of light microscope images. The porosity concentration were $0.07 \pm 0.02\%$ (high quality; 500 mm/s; 79 J/mm^3), $0.3 \pm 0.18\%$ (medium quality; 300 mm/s; 132 J/mm^3), and $1.42 \pm 0.85\%$ (poor quality; 800 mm/s; 50 J/mm^3). The light microscope images of the different qualities are shown in Fig. 1b–d.

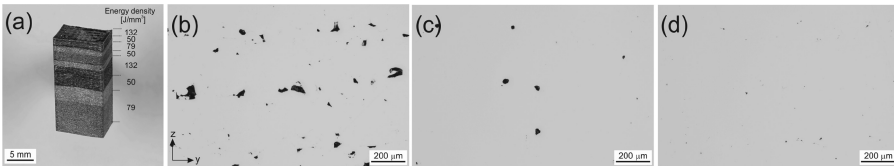


Fig. 1. (a) SLM test part produced with three energy densities where 50 J/mm^3 are bright regions, 79 J/mm^3 are dark regions and 132 J/mm^3 are blueish regions; (b) – (d) Typical light microscope cross-section images of regions produced with (a) 50 J/mm^3 , 800 mm/s, poor quality with pores concentration of $1.42 \pm 0.85\%$, (b) 132 J/mm^3 , 300 mm/s, medium quality with pores concentration $0.3 \pm 0.18\%$ and (c) 79 J/mm^3 , 500 mm/s, high quality with pores concentration of $0.07 \pm 0.02\%$.

In this study, the acoustic emission emitted during the process was recorded using a fiber Bragg gratings (FBG) during the whole manufacturing of the part. The FBG was placed inside the machine chamber, at a distance of 20 cm from the process zone. The FBG sensor was pumped with a narrow band laser irradiation at a wavelength of $1547 + 0.01 \text{ nm}$ and a light power of 4 mW. The FBG sensor provided a 50% of reflectivity in the optical read out signal and more details about FBGs can be found in [20, 21]. The reflected signal was additionally digitized using a high speed photo-diode, connected to data acquisition unit and a data recording software. Both were from Vallen (Vallen GmbH., Germany). All signals were digitized with a sampling rate of 1 MHz. As an example, the AE signal of a full high quality layer (79 J/mm^3 , 500 mm/s) is shown in Fig. 2a.

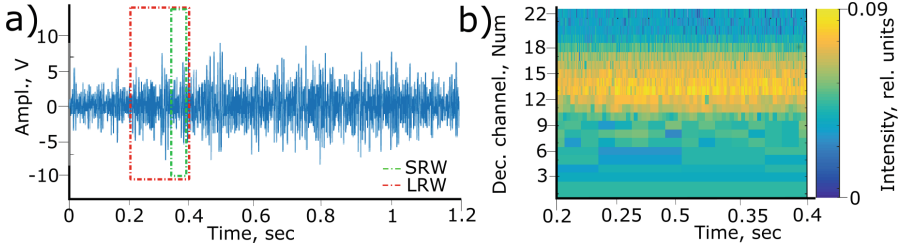


Fig. 2. (a) A typical AE signal from one complete layer of medium quality (132 J/mm^3 , 300 mm/s). LRW (red box) and SRW (green box) are the long and short running windows scanning the acquired signal; (b) the complete reconstructed spectrogram from the relative energies of the M -band wavelets for the LRW time span bounded by red lines in Fig. 2(a).

3 Data Processing

3.1 Wavelet Spectrograms

In this specific work, the search of distinct features in convolution neural network (CNN) is carried out in the time-frequency domain using wavelet spectrograms. The intensity measurement of the AE components in spectrograms was taken as the relative energies of the narrow frequency bands obtained with M -band wavelets.

M -band wavelets are extensions of the traditional wavelet transform [30, 31]. Its advantage is to operate wavelets at various signal subspaces so that they become insensitive to shift-invariance artifacts [31]. The representation of M -band wavelets as a multi-channel filtering is defined through finite impulse response filters (FIR) [31]:

$$\varphi_j(n) = \sum_n h_0(k) \sqrt{M} \varphi(Mn - k), \quad k \in \mathbb{Z} \quad (1)$$

$$\psi_{ji}(n) = \sum_n h_{m-1}(k) \sqrt{M} \psi(Mn - k), \quad k \in \mathbb{Z} \quad (2)$$

where M is the channels number, $\varphi(n)$ is a scaling function, j is the current scale, $\psi()$ is the wavelet function, h_0 , h_{m-2} , h_{m-1} are the low pass, narrow pass and high pass filters, respectively. The outcomes of Eqs. (1) and (2) are the extraction of the low, narrow and high frequency contents of the signal at a fixed scale j . This is represented by a set of decomposition coefficients $d_{j,s}$ where s denotes the shift within a single frequency band at scale j . In this contribution, the algebraic wavelets from Lin et al. [31] were used.

The use of relative energies allows tracking the energy redistribution between the different frequency bands and those are computed as:

$$\rho_{norm,j,m} = E_{j,m}/E_j \quad (3)$$

where $E_{j,m} = \int |d_{j,m}(t)|^2 dt = \sum_k |d_{j,s}|^2$ is the energy of frequency band m at scale j and E_{ij} is a summary of the energy of all frequency bands within the spectrogram. The

outcome of Eq. (3) is a spectrogram. An example of an AE signal and a spectrogram are presented in Fig. 2. The spectrogram is reconstructed from a pattern of the signal in Fig. 2a that is bounded by the red lines between 0.2 and 0.4 s.

In this investigation, two AE patterns from the AE signal were analyzed and marked in Fig. 2a by a red and green boxes. These patterns are defined as a LRW (Long Range Window, red box) and SRW (Short Range Window, green box). Both have different span time and have different purposes. The AE signals will be scanned by these two windows. The SRW will provide a higher resolution for more precise spatial localization of single process events in the future. But, its short time span makes it sensitive to noise. This problem is expected to be surmounted thank to the LRW that will be responsible for the whole classification stability. In this work, the LRW is a short term memory of a set of several previous and one current SRW.

3.2 Introduction to Wavelet Spectrograms

In this study, the CNN structure was adjusted to process the flows of the spectrograms from both the LRW and SRW, simultaneously. The scheme of the new CNN structure is presented in Fig. 3. The two spectrograms go through two separate convolution layers from which we get a series of perception maps 1. The information from those is further aggregated in the pooling layers 1. Then, the information from both flows is forwarded into the common convolution layer 2 which is followed by an additional repentence of the pooling operation (see pooling 2 in Fig. 3). The final classification is carried out in fully connected layers as schematically presented in Fig. 3. The classification result is the output of the procedure and this is given in Table 1. More details can be found in Thomas et al. [32] for the pooling operation and Krizhevsky et al. [33] for self-feature extraction and CNN operation principles.

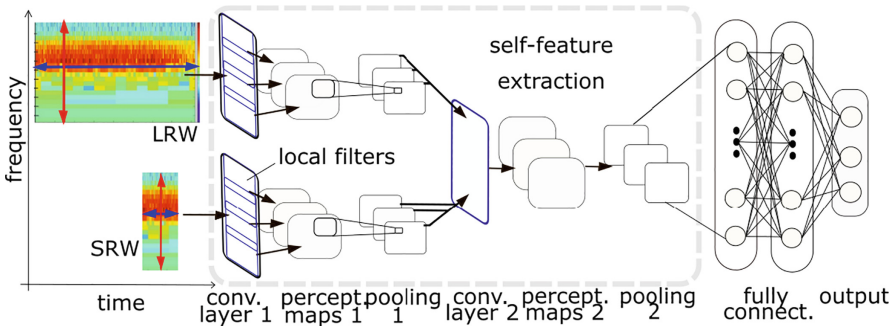


Fig. 3. The structure of the CNN, where LRW and SRW denote the long rang window and short range window, respectively.

Table 1. Test results for different categories (in rows) versus ground truth (in columns). The color intensity encodes the match of the test result to the ground truth. In brackets the classification results only for LRW/SRW are shown

Test categories \ Ground truth	Poor	Medium	High
	Poor (1.42 ± 0.85 %, 800 mm/s)	84 (84/69)	7 (8/12)
Medium (0.3 ± 0.18 %, 300 mm/s)	7 (9/10)	82 (80/63)	11 (11/27)
High (0.07 ± 0.02 %, 500 mm/s)	11 (12/18)	10 (9/21)	79 (79/61)

4 Results and Discussion

4.1 Dynamical Range

As mentioned in Sect. 2, the AM machine employed in this investigation is an industrial Concept M2. Due to their conceptions, such industrial machines have a non-negligible background noise, in particular for acoustic emission (AE). Consequently, it is of utmost importance to be able to decouple the AE of the AM process from the background noise. This was accomplished by recording the machine internal noises without the AM process. Those signals were, then, utilized for the evaluation of the noise background.

It was found from the spectrograms that the background noise of the Concept M2 machine appears in a wide spectral range as for the AM process. However, some discernible dissimilarity was discovered in the range of 9 to 15 KHz (not shown here).

The noise reduction in the industrial mechanic systems are well known and can be effectively suppressed by design of filters. These noises are mainly characterized by low frequencies [34]. But, in this current study, we relied on the ability of CNN to suppress the stationary noises.

4.2 Classification Results

The training dataset included in total 1.200 LRWs and 4.800 SRWs from the three quality categories, which were extracted from the AE signals. In this dataset, each category had the same number of signals. After the training, to test the data, we used a different dataset that was not used in the training procedure. This can be assimilated to newly data recorded for a new part. The test dataset was also constituted by the same number of LRWs and SRWs for each category.

The accuracies of the classification results using the test dataset are given in Table 1. In this table, the numbers without brackets represent the total accuracies (LRW and SRW). The numbers in brackets are the classification results for only either the LRW or the SLRW, respectively. The ground truths, in this table, are given in the columns whereas the classification test categories are in rows. The accuracy is calculated from the number of the true positives divided by the total number of the tests for the individual categories. The total accuracies achieved using the aforementioned time spans for both windows lie between 79 and 84%. The classification errors for each category correspond to the values in the non-diagonal cells of Table 1. For example,

the AE test data from poor quality was classified with an accuracy rate of 84% and so it has the lowest error rate. The classification error is the lowest (7%) for the medium quality and the highest (9%) for the highest quality. The situation is completely inverted for the medium quality. Finally, the classification error, for the high quality, is almost the same for medium and poor quality.

We would like to point out again here that the poorest quality is made with the highest speed (800 mm/s), followed by the high quality (500 mm/s) and finally the medium quality (300 mm/s). It is also interesting to note that, for the poor quality, the error rates decrease as the differences in the laser scanning speed increases. In contrast, this statement is not valid for the medium quality. In this case, the error rate is highest for the high quality, although the laser scanning speed difference is the smallest as compared to the poor quality, and the error rate is lowest for the poor quality, despite having the largest laser scanning speed difference. As far as the high quality is concerned, although the error rates between the two other quality levels, the lowest value is found to be for the medium quality (10%, 300 mm/s) which has, actually, the closest laser scanning speed with the high quality (500 mm/s) as compared to the poor quality (11%, 800 mm/s). Hence, we can conclude that the laser scanning velocity has no impact on the self-extraction of the distinct features in CNN.

Another source of error may be due to the acoustic echo and noise behavior produced during the additive process. As already mentioned, there are some overlaps in the AE signals coming from the AM process and the noise of the machine. Considering also the stochastic behavior of the AM process and the noise of the machine, it cannot be excluded that some features are not well classified during the training. Such behaviors complicate the extraction of the distinct frequencies and increase the error rates.

The results of the AE signal classification for the LRW and SRW only are presented in brackets in Table 1. It is found that the classification accuracy obtained only considering the LRW is very close or equal to the total classification accuracy, which is obtained from the combined LWR and SRW. In contrast, the classification accuracy of the SRW only is significantly lower than the total and LRW only accuracies. Two reasons may account for this result. First, this may be due to the fact that the SRWs are extremely sensitive to the noises as they operate at much smaller time scales. Second, this could be due to the fluctuations of the acoustic signal from the additive process. The local fluctuations might be caused by very local events which are different from each other due to the non-uniformities of the laser-material interactions. Those are probably caught by the SRWs due to their much smaller time scales. This conveys to higher error rates when splitting all signals only in three categories. Despite its poor classification accuracy, the SRW will bring benefits in the future. Due to the shorter time spans, we will be able to localize more precisely the defects. But, this was out of the scope of this contribution and is the subject for further developments.

5 Conclusions

The main goal of this contribution was to study the feasibility of a very innovative approach which combines acoustic emission (AE) with artificial intelligence (AI) for *in situ* and real-time monitoring of additive manufacturing (AM) processes.

To answer the question, we used an industrial selective laser melting (SLM) machine Concept M2. The material used was a CL20ES stainless steel (1.4404/316L) powder (\varnothing 10–45 μm). The acoustic sensor selected was a fiber Bragg grating (FBG) due to its high sensitivity. In terms of artificial intelligence, a convolution neural network (CNN) was employed. The CNN employed was modified to be able to analysis input data at two time scales. The CNN was fed with wavelet spectrograms that were are a representation of the AE signals. A part was produced with constant process parameters except for the laser scanning velocity. Three laser scanning speeds were selected to give three levels of quality levels in terms of porosity. The measured porosity concentration were $0.07 \pm 0.02\%$ (high quality; 500 mm/s; 79 J/mm³), $0.3 \pm 0.18\%$ (medium quality; 300 mm/s; 132 J/mm³), and $1.42 \pm 0.85\%$ (poor quality; 800 mm/s; 50 J/mm³). The recorded AE signals were grouped accordingly.

It is known that industrial machines, such as the Concept M2 machine, produce high noise levels resulting in a low signal/noise ratio leading to classification inaccuracies. The approach considered in this work has two tools for effective noise suppression. To start with, we used wavelet spectrograms which allow suppressing noises by excluding the noisy frequency bands. Secondly, the noises can be partly eliminated by the artificial intelligence framework during the training procedure.

The CNN was trained and tested on two different datasets. The classification accuracy was in the range of 79–84%. It was also found that the long range window (LRW) had a very close classification accuracy as compared to the total classification accuracy. The results of the short range window (SRW) are much lower than the LRW and this was explained by the fact that SRW was very sensitive to the local fluctuations of the AE signals.

To conclude, our results show that there are distinct AE features for each manufacturing quality. The extracted features can be differentiated with artificial intelligence technique. Taking into account that it is the first tests carried out, the classification results can be considered as very promising and they showed the feasibility of the quality monitoring of AM process by combining acoustic emission and artificial intelligence.

For improving our actual algorithm to deal with very noisy atmosphere, it requires additional investigation of noises nature and types. Moreover, a further increase of the sensitivity of the AE sensor is possible by utilizing other optical structures. Both ameliorations are our future work.

References

1. Guo, N., Leu, M.: Additive manufacturing: technology, applications and research needs. *Front. Mech. Eng.* **8**(3), 215–243 (2013). doi:[10.1007/s11465-013-0248-8](https://doi.org/10.1007/s11465-013-0248-8)
2. Wohlers Report – 3D Printing and Additive Manufacturing State of the Industry. Annual Worldwide Progress Report. Wohlers Associates, 2013–2016
3. Gu, D.D., Meiners, W., Wissenbach, K., Poprawe, R.: Laser additive manufacturing of metallic components: materials, processes and mechanisms. *Int. Mat. Rev.* **57**, 133–164 (2012). doi:[10.1179/1743280411Y.0000000014](https://doi.org/10.1179/1743280411Y.0000000014)

4. Huang, S.H., Liu, P., Mokasdar, A., Hou, L.: Additive manufacturing and its societal impact: a literature review. *Int. J. Adv. Manuf. Tech.* **7**, 1191–1203 (2013)
5. Zhai, Y.W., Lados, D.A., Lagoy, J.L.: Additive manufacturing: making imagination the major limitation. *JOM* **66**, 808–816 (2014)
6. Khairallah, S.A., Anderson, A.T., Rubenchik, A., King, W.E., Livermore, L.: Laser powder-bed fusion additive manufacturing: physics of complex melt flow and formation mechanisms of pores, spatter, and denudation zones. *Acta Mat.* **108**, 36–45 (2016). doi:[10.1016/j.actamat.2016.02.014](https://doi.org/10.1016/j.actamat.2016.02.014)
7. Gibson, I., Rosen, D.W., Stucker, B.: Additive manufacturing technologies, rapid prototyping to direct digital manufacturing. Springer Science + Business Media (2010). [10.1007/978-1-4419-1120-9](https://doi.org/10.1007/978-1-4419-1120-9)
8. Frazier, W.E.: Metal additive manufacturing: a review. *J. Mater. Eng. Perform.* **23**, 1917–1928 (2014). doi:[10.1007/s11665-014-0958-z](https://doi.org/10.1007/s11665-014-0958-z)
9. King, W.E., Anderson, A.T., Ferencz, R.M., Hodge, N.E., Kamath, C., Khairallah, S.A., Rubenchik, A.M.: Laser powder bed fusion additive manufacturing of metals; physics, computational, and materials challenges. *Appl. Phys. Rev.* **2**, 041304 (2016). doi:[10.1063/1.4937809](https://doi.org/10.1063/1.4937809)
10. Tammas-Williams, S., Zhao, H., Léonard, F., Derguti, F., Todd, I., Prangnell, P.B.: XCT analysis of the influence of melt strategies on defect population in Ti–6Al–4 V components manufactured by selective electron beam melting. *Mater. Charact.* **102**(4), 47–61 (2015). doi:[10.1016/j.matchar.2015.02.008](https://doi.org/10.1016/j.matchar.2015.02.008)
11. Shifeng, W., Shuai, L., Qingsong, W., Yan, C., Sheng, Z., Yusheng, S.: Effect of molten pool boundaries on the mechanical properties of selective laser melting parts. *J. Mater. Process. Tech.* **214**(11), 2660–2667 (2014). doi:[10.1016/j.jmatprotec.2014.06.002](https://doi.org/10.1016/j.jmatprotec.2014.06.002)
12. Everton, S.K., Hirsch, M., Stravroulakis, P., Leach, R.K., Clare, A.T.: Review of in-situ process monitoring and in-situ metrology for metal additive manufacturing. *Mat. Des.* **95**, 431–445 (2016). doi:[10.1016/j.matdes.2016.01.099](https://doi.org/10.1016/j.matdes.2016.01.099)
13. Tapia, G., Elwany, A.: A review on process monitoring and control in metal-based additive manufacturing. *J. Manuf. Sci. Eng.* **136**, 10 (2014). doi:[10.1115/1.4028540](https://doi.org/10.1115/1.4028540)
14. Herzog, F., Bechmann, F., Berumen, S., Kruth, J.P., Craeghs, T.: Inventors method for producing a three-dimensional component patent WO1996008749 A3, 2013, 23 August 1995
15. Vaidya, R., Anand, S.: Image processing assisted tools for pre- and post-processing operations in additive manufacturing. *Proc. Manuf.* **5**, 958–973 (2016). <http://dx.doi.org/10.1016/j.promfg.2016.08.084>
16. Alhwarin, F., Ferrein, A., Gebhardt, A., Kallweit, S., Scholl, I., Tedjasukmana, O.: Improving additive manufacturing by image processing and robotic milling. In: *IEEE Int. Conf. Autom. Sci. Eng. (CASE)* 24–28 August, pp. 924–929 (2015). doi:<https://doi.org/10.1109/CoASE.2015.7294217>
17. Furumoto, T., Alkahari, M.R., Ueda, T., Aziz, M.S.A., Hosokawa, A.: Monitoring of laser consolidation process of metal powder with high speed video camera. *Phy. Proc.* **39**, 760–766 (2012). doi:[10.1016/j.phpro.2012.10.098](https://doi.org/10.1016/j.phpro.2012.10.098)
18. Furumoto, T., Ueda, T., Alkahari, M.R., Hosokawa, A.: Investigation of laser consolidation process for metal powder by two-color pyrometer and high-speed video camera. *CIRP Ann. Manuf. Technol.* **62**, 223–226 (2013). doi:[10.1016/j.cirp.2013.03.032](https://doi.org/10.1016/j.cirp.2013.03.032)
19. Wu, H., Yu, Z., Wang, Y.: A new approach for online monitoring of additive manufacturing based on acoustic emission. In: *ASME 2016 11th International Manufacturing Science and Engineering, Conference Paper No. MSEC2016–8551, V003T08A013*, pp. 1–8 (2016) doi:[10.1115/MSEC2016-8551](https://doi.org/10.1115/MSEC2016-8551)
20. Kashyap, R.: *Fiber Bragg Grating*, 2nd edn. Elsevier, Amsterdam (2010). ISBN 978-0-12-372579-0

21. Ramakrishnan, M., Rajan, G., Semenova, Y., Farrell, G.: Overview of fiber optic sensor technologies for strain/temperature sensing applications in composite materials. *Sensors* **16**(1), 99 (2016). doi:[10.3390/s16010099](https://doi.org/10.3390/s16010099)
22. Grosse, C.U., Ohtsu, M.: *Acoustic emission testing*. Springer-Verlag, Berlin, Heidelberg. doi:[10.1007/978-3-540-69972-9](https://doi.org/10.1007/978-3-540-69972-9)
23. Sharratt, B.M.: Non-destructive techniques and technologies for qualification of additive manufactured parts and processes: a literature review, Contract Report DRDC-RDDC-2015-C035 (2015). http://cradpdf.drdc-rddc.gc.ca/PDFS/unc200/p801800_A1b.pdf
24. Cerniglia, D., Scafidi, M., Pantano, A., Łopatka, R.: Laser ultrasonic technique for laser powder deposition inspection. In: 13th International Symposium on Non-dest. Charact. Mat., Le Mans, May 2013. http://www.ndt.net/article/ndcm2013/content/papers/13_Cerniglia.pdf
25. Purtonen, T., Kalliosaari, A., Salminen, A.: Monitoring and adaptive control of laser processes. *Phys. Proc.* **56**, 1218–1231 (2014). doi:[10.1016/j.phpro.2014.08.038](https://doi.org/10.1016/j.phpro.2014.08.038)
26. Strantz, M., Aggelis, D.G., de Baere, D., Guillaume, P., van Hemelrijck, D.: Evaluation of SHM system produced by additive manufacturing via acoustic emission and other NDT methods. *Sensors* **15**, 26709–26725 (2015). doi:[10.3390/s151026709](https://doi.org/10.3390/s151026709)
27. Shevchik, S.A., Kenel, C., Leinenbach, C., Wasmer, K.: Acoustic emission quality monitoring in additive manufacturing using spectral convolutional neural networks. Submitted in *Add. Manf.* (s2017)
28. Schmidhuber, J.: Deep learning in neural networks: an overview. *J. Neural. Netw.* **61**, 85–117 (2015). doi:[10.1016/j.neunet.2014.09.003](https://doi.org/10.1016/j.neunet.2014.09.003)
29. Thijs, L., Verhaeghe, F., Craeghs, T., Humbeeck, J.V., Kruth, J.P.: A study of the microstructural evolution during selective laser melting of Ti–6Al–4 V. *Acta Mater.* **58**(9), 3303–3312 (2010). doi:[10.1016/j.actamat.2010.02.004](https://doi.org/10.1016/j.actamat.2010.02.004)
30. Daubechies, I.: Ten lectures on wavelets. In: CBMS-NSF Regional Conference Series in Applied Mathematics (1992) [10.1137/1.9781611970104](https://doi.org/10.1137/1.9781611970104)
31. Lin, T., Xu, S., Shi, Q., Hao, P.: An algebraic construction of orthonormal M-band wavelets with perfect reconstruction. *Appl. Math. Comput.* **172**(2), 717–730 (2006). doi:[10.1016/j.amc.2004.11.025](https://doi.org/10.1016/j.amc.2004.11.025)
32. Thomas, S., Ganapathy, S., Saon, G., Soltau, H.: Analyzing convolutional neural networks for speech activity detection in mismatched acoustic conditions, Acoustics, Speech and Signal Processing (ICASSP). In: IEEE International Conference on Acoustics Speech and Signal Processing (ICASSP) (2014). [10.1109/ICASSP.2014.6854054](https://doi.org/10.1109/ICASSP.2014.6854054)
33. Krizhevsky, A., Sutskever, I., Hinton, G.E.: ImageNet classification with deep convolutional neural networks. *Adv. Neur. Inf. Proc. Sys.* **25** (NIPS 2012) (2012). <https://papers.nips.cc/paper/4824-imagenet-classification-with-deep-convolutional-neural-networks>
34. Crocker, M.J. (ed.): *Handbook of Noise and Vibration Control*. Wiley, New Jersey (2007). doi:[10.1121/1.2973236](https://doi.org/10.1121/1.2973236). ISBN 978-0-471-39599-7